

# Performances and results on the sky of the NAOS visible wavefront sensor

Philippe Feautrier<sup>a</sup>, Gérard Rousset<sup>b</sup>, Reinhold J. Dorn<sup>c</sup>, Cyril Cavadore<sup>c</sup>, Julien Charton<sup>a</sup>, Claudio Cumani<sup>c</sup>, Thierry Fusco<sup>b</sup>, Norbert Hubin<sup>c</sup>, Pierre Kern<sup>a</sup>, Jean-Louis Lizon<sup>c</sup>, Yves Magnard<sup>a</sup>, Pascal Puget<sup>a</sup>, Didier Rabaud<sup>b</sup>, Patrick Rabou<sup>a</sup> and Eric Stadler<sup>a</sup>.

<sup>a</sup> LAOG: Laboratoire d'Astrophysique de Grenoble, BP 53, 38041 Grenoble Cedex 9, France.

<sup>b</sup> ONERA: Office National d'Etudes et de Recherches Aérospatiales, France.

<sup>c</sup> ESO: European Southern Observatory, Germany and Chile

## ABSTRACT

The NAOS adaptive optics system was installed in December 2001 on the Nasmyth focus of the ESO VLT. It includes two wavefront sensors: one is working at IR wavelengths and the other at visible wavelengths. This paper describes the NAOS Visible Wave Front Sensor based on a Shack-Hartmann principle and its performances as measured on the sky. This wavefront sensor includes within a liquid nitrogen continuous flow cryostat:

1) a low noise fast readout CCD camera controlled by the ESO new generation CCD system FIERA using a fast frame rate EEV/Marconi CCD-50 focal plane array. This 128x128 pixels focal plane array has a readout noise of 3 e<sup>-</sup> at 50 kilopixel/sec/port. FIERA provides remotely controlled readout modes with optional binning, windowing and flexible integration time.

2) two remotely exchangeable micro-lens arrays (14x14 and 7x7 micro-lenses) cooled at the CCD temperature ( -110 °C). The CCD array is directly located in the micro lenses focal plane at a few millimeters apart without relay optics.

Additional opto-mechanical functions are also provided (atmospheric dispersion compensator, flux level control, field of view limitation).

On sky performances of the wavefront sensor are presented. Adaptive Optics corrections was obtained with a reference star as faint as a visible magnitude 17.

Keywords: CCD, low noise, camera, adaptive optical system, wavefront sensor, Strehl Ratio, microlenses, cryostat.

## 1. INTRODUCTION

NAOS, fully described in Ref. 1 and Ref.2 , is the Adaptive Optics (AO) system of the ESO Very Large Telescope (see Figure 1, left). Installed at the Nasmyth focus of the VLT, NAOS is the AO system for CONICA (see Ref.3 ), the science infrared camera in the 1-5  $\mu\text{m}$  wavelengths range. NAOS provides diffraction limited images at K band for average seeing conditions. NAOS has been designed and manufactured by a French consortium (ONERA, LAOG and Observatoire de Paris).

The deformable mirror with 185 useful actuators compensates the atmospheric disturbance measured by the two Shack Hartmann wave-front sensors (WFS), one covering the visible wavelengths range and the other covering the infrared. This paper describes the visible wave front sensor and its CCD camera. NAOS is mounted on the telescope adapter rotator and rotates with the telescope field rotation. Therefore, the structure stiffness of the whole instrument is a big issue for the final performances of the instrument. The opto-mechanical path of the wave-front sensing channel requires a special care to avoid flexure contribution to the measurements which may highly contribute to an image quality degradation.

The sensitivity of the whole NAOS instrument is highly dependent of the wave-front sensor performances. The visible WFS for NAOS uses a 128x128 pixels low noise CCD manufactured by EEV/Marconi with 16 output ports to allow a

high frame rate (up to 500 frames/sec) and low noise ( $3 e^-$ ). The whole camera (see Figure 1, right) and the CCD performances are described in this paper.

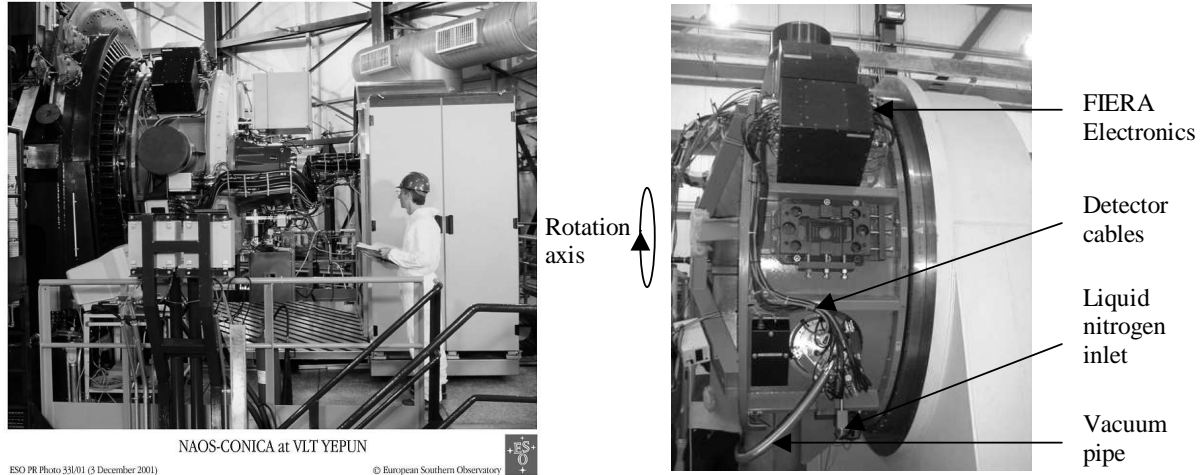


Figure 1: NAOS-CONICA view mounted on the Yepun telescope (left) and the CCD camera system mounted on the NAOS adapter during the integration period in Paranal (right).

## 2. THE VISIBLE WAVEFRONT SENSOR

The Visible WFS consists in two main parts:

- The opto-mechanical bench.
- The CCD camera head including the micro-lens directly mounted in front of the CCD.

The spectral range used for the visible wavefront sensor is 0.45 to 1  $\mu\text{m}$ . It corresponds to the optimization of the optical train and of the coatings.

The Figure 2 is a block diagram of the NAOS visible WFS:

A dichroic beam splitter shares the NAOS incoming light between the scientific path (CONICA) and the wave-front sensing path. The reflected part of the light is redirected to the wave-front sensors.

A Field Selector, composed of two parallel mirrors placed in the F/15 beam in telecentric condition, chooses the reference star for wave-front sensing apart from the scientific observed object. This system can take a reference star within a  $\pm 1$  arcmin field of view. This very critical sub-system must insure a strong stability compatible with the NAOS servo loop. Both mirrors of the field selector must provide a sub-arcsecond mechanical stability over its  $\pm 6^\circ$  mechanical angular amplitude. Then a mirror selects the required wave-front sensor, either IR or visible WFS.

In the visible wavefront sensor optical train, a first collimator images the pupil on the Atmospheric Dispersion Compensator (ADC).

Neutral density filter can be introduced for reference source brightness adaptation, in order to provide the required 100,000 dynamic which is larger than the dynamic of the detector. Three transmissions are selectable (no density, 1/20 and 1/400 transmission).

The ADC is required to enhance WFS accuracy when zenith angle increases by compensating elongation due to the atmospheric dispersion in the spectral band.

Focusing lens allows to image a focal plane on the field stop diaphragm.

The stop adapts the field of view of the wave-front sensor for each micro-lens configuration. It is required to avoid micro-lens field's superposition on the detector. Three fields and a blocking positions are available.

The "pupil image lens" images the pupil on the micro-lens array inside the cryostat. Images are formed directly on detector by the micro-lenses. The two micro-lenses are on the same substrate and can be exchanged in front of the detector, thanks to a cooled translation mechanism. The micro-lens holder allows 3 positions: 14x14 array, 7x7 array and free position for pupil imaging. This holder is a critical point of the design according to the stability requirement (i.e. 0.1  $\mu\text{m}$  for a  $30^\circ$  rotation of the NAOS adapter).

All displacements are remotely controlled. In this concept, we choose to avoid displacements of optical parts influencing the optical alignments, except for the micro-lens holder.

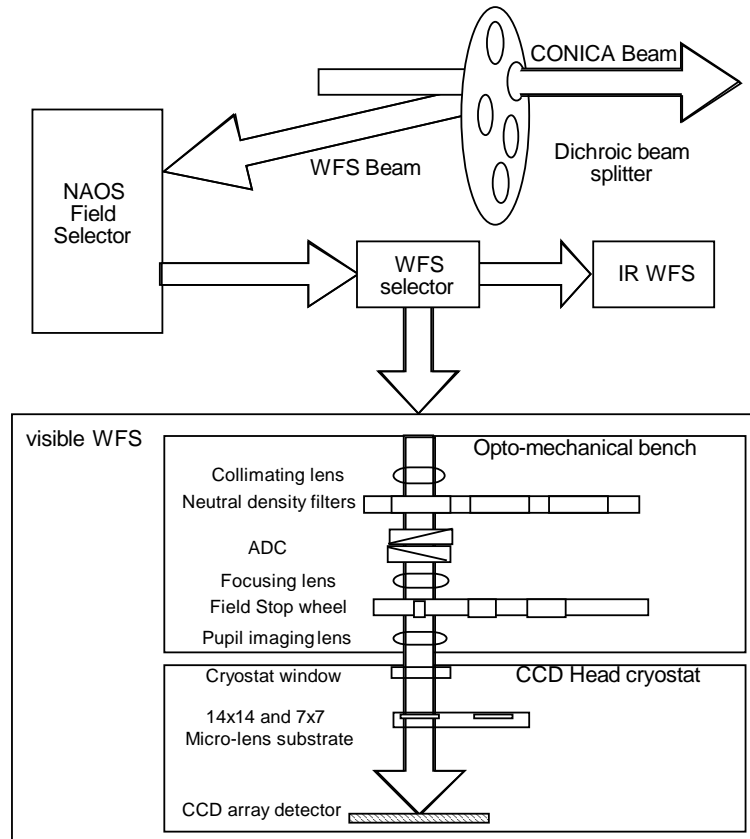


Figure 2: Block diagram of NAOS and the visible wave-front sensor.

The visible wave-front sensor has the configuration capabilities according to the micro-lens choice given in Table 1. The focal length is the same for the 2 arrays. The pixel field of view under-samples the sub-aperture diffraction pattern, because the sub-aperture size is much larger than the field diameter for the wavelength range of the wave-front sensor. The total field of view per sub-aperture is small in the 14x14 configuration in order to minimize the readout noise influence in the centroid measurement.

Lenslet array configuration	<b>14 x 14</b>	<b>7 x 7 (x2 binning)</b>
Focal length	5.75 mm	5.75 mm
Micro-lens diameter	192 $\mu$ m	384 $\mu$ m
Pixel Field of View	0.29"	0.58"
Micro-lens Field of View	2.32"	4.64"
Diaphragm diameter	1.066 mm	2.131 mm
Number of pixels per sub-aperture	8 pixels	8 pixels (binning 2)
WFS pupil diameter	2.688 mm	2.688 mm
Image core central diameter	38 $\mu$ m	19 $\mu$ m

Table 1 : main characteristics of the 2 lenlet arrays configurations

### 3. THE LOW NOISE FAST READOUT CAMERA

#### 3.1 THE EEV/MARCONI CCD-50 DESCRIPTION AND ARCHITECTURE

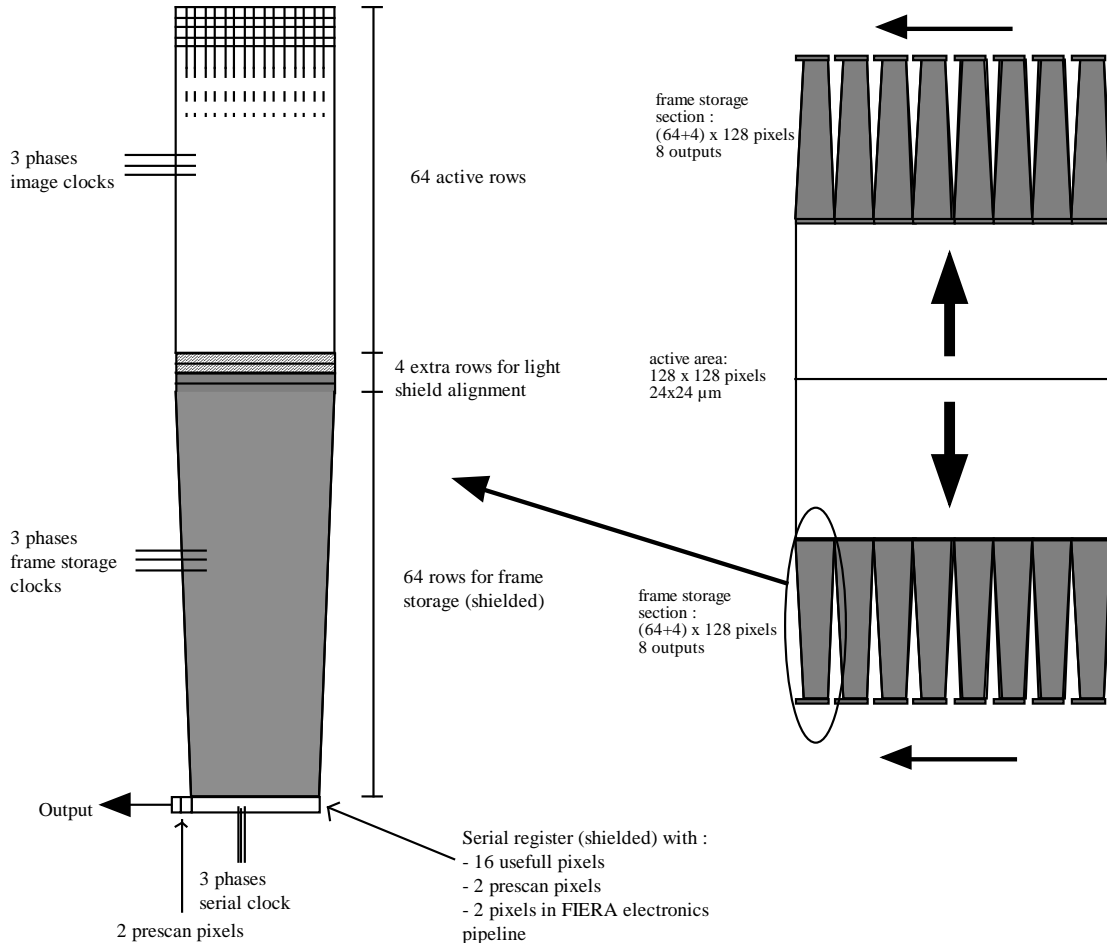


Figure 3: detector architecture of the 128x128 CCD .

The CCD used in the NAOS project was manufactured by EEV/Marconi under an ESO contract.

This CCD is a split frame transfer CCD with a light sensitive area of 128x128 pixels and a pixel size of 24  $\mu\text{m}$ . The 2 storage sections are light shielded. Additional 4 rows on each storage section compensates if the light shield is misaligned. The charge is shifted to each 8 output amplifiers on the bottom and top side. Therefore, the CCD is partitioned into 16 sections with one amplifier per section (see Figure 3).

A subsection of the CCD chip with 16 x 64 pixels of the image zone, the corresponding storage section and the serial register are also shown on this figure. All of these sections of the CCD will be clocked in exactly the same way.

Because of the lenslet array configuration (14x14 or 7x7 sub-apertures), only 14 of the 16 CCD outputs are used for NAOS.

The Quantum Efficiency of the CCD is very high in all the visible wavelengths and is presented in the Figure 4:

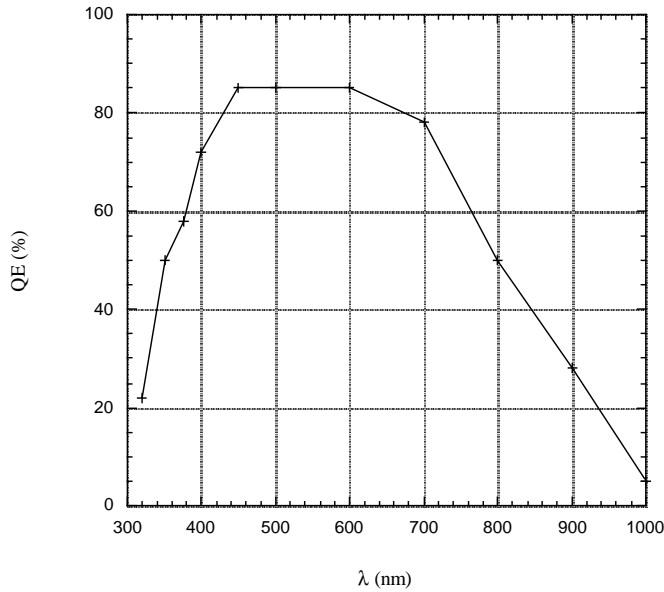


Figure 4: Quantum Efficiency of the CCD detector EEV/Marconi CCD-50.

## 3.2 THE FIERA CCD CONTROLLER

### 3.2.1 PRESENTATION

ESO has built an universal CCD controller able to drive a variety of "new generation" CCD. This original system is called FIERA (Fast Imager Electronic Readout Assembly), see Ref. 5. The requirements for the FIERA CCD Controller are briefly summarized hereafter:

- System noise negligible compared to the readout noise of the CCD amplifier.
- x2 and x4 binning capability, windowing capability
- Up to 2 Mpixel/sec operation
- 16 simultaneous video outputs can be managed. On NAOS, we use 14 A/D converters 16 bits/1 MHz
- Cross-talk between channels of the CCD controller must be negligible - less than 1 bit or less than the CCD readout noise.

### 3.2.2 THE CCD READOUT MODES AND NOISE PERFORMANCES

Each readout mode defines the following parameters: windowing, binning, conversion gain (in e-/adu), frame rate.

We need several readout mode for the following reasons:

- we have to match the readout mode with the micro-lens array configuration (7x7 or 14x14 micro-lenses)
- the readout noise has a strong impact on the NAOS performance in terms of sky coverage, we need to decrease it as much as possible. Because the readout noise decreases with the pixel frequency, the CCD readout is designed to skip the unused pixels, either by binning or by windowing. Then the pixel frequency can be reduced. The Table 2 shows the list of readout modes that are effectively used in NAOS. Also shown in this table are the noise of the CCD camera measured on the VLT telescope, demonstrating the very low noise performances of this system.

Mode Number	Pixel rate (kpixels/s)	Gain (adu/e-)	Measured Noise (e-)	Binning	Windowing	Max Frame Rate (Hz)
1	280	0.34	3.9	1x1	No	209
2	635	0.33	5.4	1x1	No	444
3	635	2.1	6.9	1x1	No	444
4	280	0.35	3.9	1x1	6x6	277
5	50	0.34	2.9	2x2	No	136
6	280	0.36	4.3	2x2	No	587
7	50	0.34	2.98	2x2	6x6	133
8	50	0.34	2.92	4x4	No	383

Table 2: List of readout modes for the NAOS visible wave-front sensor and readout noise performances measured on the VLT telescope.

The readout noise vary from 2.9 e- at a pixel rate of 50 kpixels/sec to 5.4 e- at a pixel rate of 635 kpixels/sec with the high gain configuration (0.3 adu/e-). This allows to have frame rate between 133 to 444 Hz. From the 8 basic modes, 48 readout modes are derived with increased integrating time obtained with an additional gap between 2 image readout, covering a frame rate range of 15 to 444 Hz.

Using the maximum frame rate (444 Hz) of the CCD, the maximum achievable bandwidth at 0 dB of the so-called open-loop transfer function of the adaptive optic servo-loop is 35 Hz, as measured in laboratory. This bandwidth is mainly limited by the frame rate of the CCD.

### 3.3 CRYOSTAT FLEXURES

The specifications concerning the cryostat flexures when this one is rotated are very strict. Flexure tests was performed using a rotating table allowing a full 360° rotation to simulate the NAOS adapter rotation during the astronomical observations on the telescope.

Cryostat flexures as low as 2 microns (peak to peak for one complete turn) of the inner part of the cryostat compared to the outer part was measured and 0.1 microns in the same conditions for the micro-lenses displacement compared to the CCD, demonstrating a remarkable stiffness of the cryostat and of the micro-lens arrays exchange mechanism (see Ref. 6).

### 3.4 LENSLET ARRAY ALIGNMENT

The 2 lenslet arrays are aligned compared to the CCD with the following specifications :

- X and Y lenslet location (/CCD) accuracy : 2  $\mu\text{m}$
- parallelism CCD/lenslet array : 2  $\mu\text{m}$  from one side of the lenslet to the other

An image of the aligned spots obtained at cold temperature with the 2 lenslet arrays is shown in the Figure 5. From these images, we computed the location of each spot by measuring the centroid of each spot and we deduced the overall lenslet alignment accuracy in location and parallelism.

The two lenslet arrays can be exchanged at cold temperature with a re-positioning precision of 2  $\mu\text{m}$  (RMS).

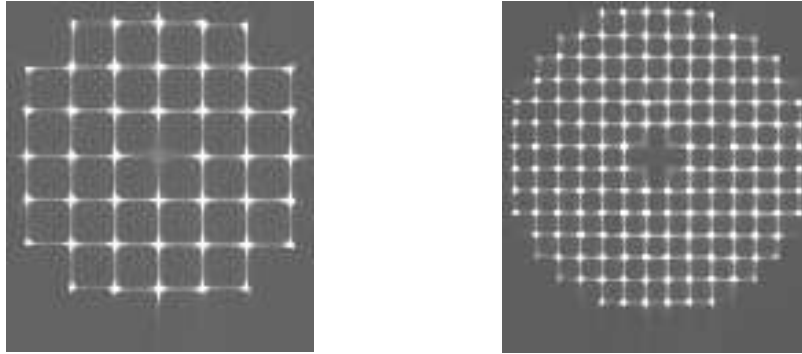


Figure 5: (right) image of the spots with the 14x14 lenslet array at cold temperature, micro-lenses aligned; (left) same image with the 7x7 lenslet array.

#### 4. RESULTS ON THE VLT TELESCOPE

NAOS, including all its subsystems like the visible wavefront sensor, was installed on the VLT *Yepun* telescope unit by mid-november 2001, as well as the scientific infrared camera CONICA. NAOS and CONICA obtained their first light on the VLT by November 25<sup>th</sup> 2001 during the first commissioning period. The excellent performances of NAOS and of the visible wavefront sensor allows very high Strehl ratio as it is shown in the Figure 6 (see Ref. 2 for more details):

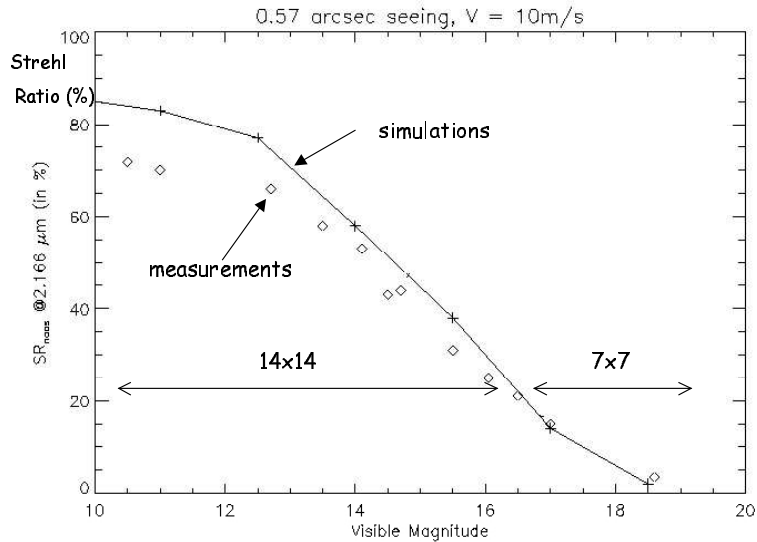


Figure 6: Strehl Ratio of NAOS and CONICA using the visible wavefront sensor . Simulations and measurements in the laboratory are shown at the same time in the figure, as well as the micro-lenses configuration (7x7 or 14x14). The seeing was 0.57 arcsec, the wind speed 10 m/s, and the Strehl Ratio is measured using a narrow band filter at 2.166  $\mu\text{m}$  with the CONICA science camera.

At low visible magnitude, Strehl Ratio up to 70% can be obtained in laboratory, whereas close-loop AO operation was demonstrated with natural guide star as faint as magnitude 17, as shown in the Figure 7. These two properties (High Strehl ratio and close-loop with very faint stars) demonstrate the remarkable qualities of the NAOS visible wavefront sensor and of its CCD camera.

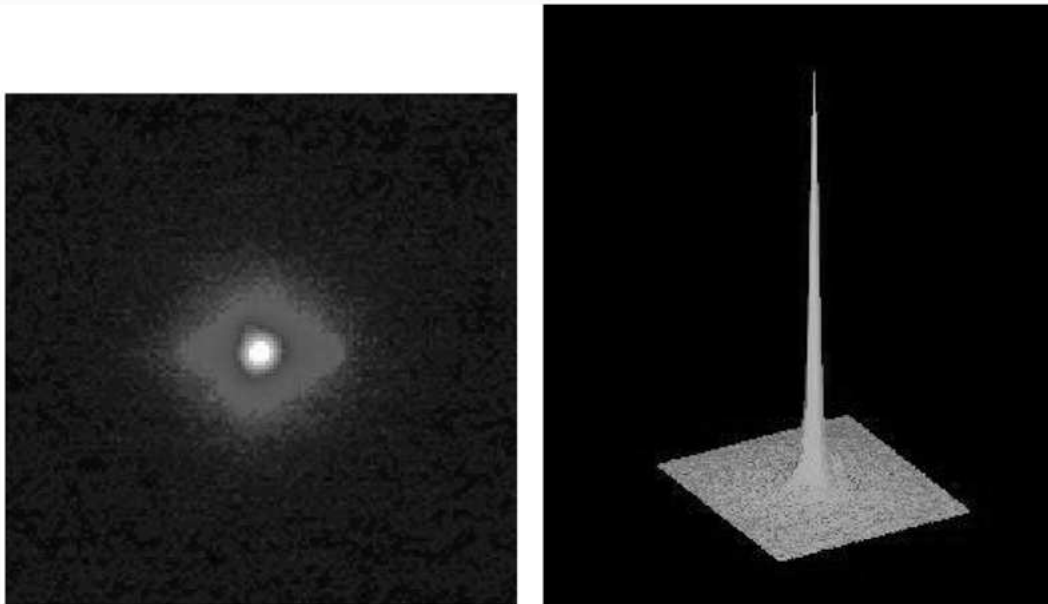


Image of a 17-mag Reference Star  
(VLT YEPUN + NAOS-CONICA)

ESO PR Photo 33i/01 (3 December 2001)

© European Southern Observatory



Figure 7: with the visible wavefront sensor, NAOS was able to close the loop using a 17-magnitude reference star just one week after the NAOS first light on the VLT (November 25, 2001).

## 5. CONCLUSION

The NAOS visible wavefront sensor, based on the Shack-Hartmann principle, was built in a strong collaboration between the ESO Optical Detector Team, the Observatory of Grenoble and ONERA. It demonstrated excellent performances due to the simultaneous qualities of the EEV/Marconi CCD chip, of the ESO/FIERA camera and of mechanical stiffness: despite of the possibility to exchange remotely the 2 lenslet arrays on the sky inside the cryostat at cold temperature, the mechanical properties of the wavefront sensor in term of stiffness and re-positioning accuracy are remarkable. Also the possibility to associate a very low readout noise with fast frame rates gives to the NAOS AO system the possibility to have high Strehl ratios and to close the loop with very faint reference stars increasing the sky coverage with visible natural guide stars. NAOS will be offered very soon to the astronomical community by autumn 2002.

## ACKNOWLEDGMENTS

These development are funded by ESO under contract number 49632/ESO/INS/95/7454/GWI. Additional funds are provided in France by INSU/CNRS and ONERA. The authors are grateful to all the colleagues involved in that project at LAOG (Grenoble), Observatoire de Paris/Meudon, ONERA and ESO.



## REFERENCES

1. G. Rousset *et al.*, "Status of the VLT Nasmyth Adaptive Optics System (NAOS)", SPIE's proceedings Astronomical Telescope and Instrumentation 2000, 27-31 March, Munich, Germany.
2. G. Rousset *et al.*, "the first AO system of the VLT: on-sky performance", this conference, SPIE's proceedings Astronomical Telescope and Instrumentation, 22-28 August 2002, Waikoloa, Hawaii, USA.
3. R. Lenzen, R. Hofmann, P. Bizenberger, "CONICA: the high resolution NIR camera for the ESO VLT", in infrared Astronomical instrumentation, A.M. Fowler, ed., Proc. SPIE 3354, paper 44, 1998.
4. L. Zago *et al.*, "NAOS Field Selector", SPIE's proceedings Astronomical Telescope and Instrumentation 2000, 27-31 March, Munich, Germany.
5. C. Cavadore and R. Dorn, "Charged Coupled Devices at the European Southern Observatory Performances and results", 4<sup>th</sup> ESO CCD Workshop, European Southern Observatory, Garching by Munchen, Germany, 13-16 September, 1999.
6. P. Feautrier *et al.*, "The NAOS visible wavefront sensor", SPIE's proceedings Astronomical Telescope and Instrumentation 2000, 27-31 March, Munich, Germany.